American Heart Association

Learn and Live

Circulation

Circulation Home ▪ Subscriptions ▪ Archives ▪ Feedback ▪ Authors ▪ Help ▪ AHA Journals Home

« Previous Article | Table of Contents | Next Article »

Articles

Regional Heterogeneity of Human Myocardial Infarcts Demonstrated by Contrast-Enhanced MRI

Potential Mechanisms

João A. C. Lima, MD; Robert M. Judd, PhD; Ann Bazille, MD; Steven P. Schulman, MD; Ergin Atalar, PhD; Elias A. Zerhouni, MD

From the Cardiology Division, Department of Medicine, and the Division of Thoracic and Magnetic Resonance Imaging, Department of Radiology, of the Johns Hopkins Hospital, Baltimore, Md.

Correspondence to Joao A.C. Lima, MD, Assistant Professor of Medicine, Carnegie 568, Cardiology Division, Johns Hopkins Hospital, 600 N Wolfe St, Baltimore, MD 21287.

This Article

▸ **Abstract** FREE
▸ **Alert me when this article is cited**
▸ **Alert me if a correction is posted**
▸ **Citation Map**

Services

▸ **Email this article to a friend**
▸ **Similar articles in this journal**
▸ **Similar articles in PubMed**
▸ **Alert me to new issues of the journal**
▸ **Download to citation manager**
▸ **Request Permissions**

Citing Articles

▸ **Citing Articles via HighWire**
▸ **Citing Articles via Google Scholar**

Google Scholar

▸ **Articles by Lima, J. A. C.**
▸ **Articles by Zerhouni, E. A.**
▸ **Search for Related Content**

PubMed

▸ **PubMed Citation**
▸ **Articles by Lima, J. A. C.**
▸ **Articles by Zerhouni, E. A.**
▸ **Pubmed/NCBI databases**
　▪ Compound via MeSH
　▪ Substance via MeSH
Medline Plus Health Information
　▪ Heart Attack

▸ ## Abstract

▲ **Top**

Background Myocardial reperfusion is pivotal to the prognosis of patients with acute myocardial infarction. In these patients, coronary flow is generally assessed by angiography and tissue perfusion by tracer scintigraphy. This study was designed to examine whether magnetic resonance imaging (MRI) provides information on myocardial perfusion and damage beyond that supplied by angiography and thallium scintigraphy after acute myocardial infarction.

Methods and Results Twenty-two patients with recent myocardial infarction had ECG, echocardiography, coronary angiography, and fast contrast-enhanced MRI. Twelve patients also had exercise thallium scintigraphy. Time-intensity curves obtained from infarcted and noninfarcted regions were correlated with coronary anatomy and left ventricular function. Two perfusion patterns were observed in infarcted regions by comparison with the normal myocardial pattern. All patients but 1 had persistent myocardial hyperenhancement within the infarcted region up to 10 minutes after contrast. In 10 patients, this hyperenhanced region surrounded a subendocardial area of decreased signal at the center of the infarcted region associated with coronary occlusion at angiography, Q waves on ECG, and greater regional dysfunction by echocardiography. Moreover, the extent and location of the MRI abnormalities correlated well with the extent and location of the fixed single-photon emission computed tomography thallium defects.

Conclusions Large human infarcts, associated with prolonged obstruction of the infarct-related artery, are characterized by central dark zones surrounded by hyperenhanced regions on MRI. Conversely, reperfused infarcts with less regional dysfunction have uniform signal hyperenhancement. The MRI hyperenhanced segment correlates well with the fixed scintigraphic defect in patients with acute myocardial infarction.

Key Words: reperfusion • edema • magnetic resonance imaging • myocardial infarction

▶ Introduction

The timing and adequacy of myocardial reperfusion largely determine the prognosis of patients with acute myocardial infarction.[1][2] When myocardial perfusion is quickly restored after coronary occlusion and maintained to the entire territory at risk, myocardial infarction may be aborted.[3] In most cases, however, only partial restoration of coronary blood flow is achieved after significant injury to the threatened segment of the left ventricular wall has already occurred.[1][2][4] Therefore, methods to evaluate the extent and adequacy of spontaneous or therapeutically induced reperfusion are necessary to assess the prognosis and management of patients with myocardial infarction.

Coronary angiography is currently the method of choice to evaluate the efficacy of reperfusion after myocardial infarction.[5] Although it reflects flow only in the large epicardial vessels and thus provides limited information on the extent of myocardial tissue reperfusion, its impact on the treatment of patients after infarction is well established.[5][6] Radionuclide scintigraphy, generally used to assess myocardial reperfusion,[7][8] is limited in terms

of spatial resolution and its dependence on both myocardial blood flow and tracer cellular uptake. The limitations of the present methods are particularly relevant in view of recent reports of incomplete myocardial reperfusion after successful thrombolysis[8] or angioplasty[9] in patients with acute myocardial infarction.

The advent of fast magnetic resonance imaging (MRI)[10] permits the acquisition of MR tomograms during a breath-hold. This creates the possibility of studying the influence of paramagnetic contrast agents on myocardial signal intensity with much greater temporal resolution[11] [12] than achieved before by spin-echo MRI. Previous experimental work using spin-echo MRI identified different contrast enhancement patterns in animals with occlusive versus reperfused infarcts.[13] [14] [15] [16] Our study was designed to examine whether, in patients with acute myocardial infarction, contrast-enhanced fast MRI provides information on myocardial perfusion and myocardial tissue damage additional to that supplied by coronary angiography and thallium scintigraphy.

In patients with acute myocardial infarction, we identified different contrast enhancement patterns that are correlated with epicardial vessel patency defined by coronary angiography and perfusion defects assessed by thallium scintigraphy. The interpretation of these enhancement patterns is based on the knowledge of the fundamental mechanisms of MR contrast enhancement defined in isolated myocardial tissue and experimental models.[13] [14] [15] [16] [17] In addition, we demonstrate that these patterns relate to the severity of acute myocardial damage modulated by attempts to restore coronary blood flow to the infarcted region.

▶ Methods

Study Patients

The study group consisted of 22 patients (16 men) with a mean age of 58 years (range, 40 to 76 years) (Table 1▣). The entry criteria included typical symptoms of acute myocardial infarction, accompanied by a creatine phosphokinase rise above two times the upper limits of normal, with an at least 5% MB band. All patients gave written informed consent according to the standards established by the Joint Committee for Clinical Investigation of the Johns Hopkins Hospital.

   View this table: **Table 1.** Clinical Characteristics of the Study Population
   [in this window]
   [in a new window]

Two-dimensional echocardiography was performed by standard techniques (Hewlett Packard Sonos 1000) in all patients within the first week after infarction. Twelve patients performed a predischarge treadmill exercise test (Naughton protocol), and at peak exercise, a dose of 3 mCi (111 MBq) of [^{201}Tl]thallium chloride was administered intravenously. Single-photon emission computed tomography (SPECT) thallium scintigraphy was performed according to our standard clinical protocol.[18] Thirty 1-minute projection images over 180° (from 45° right anterior oblique to 225° left posterior oblique) were obtained in a 64x64 matrix by use of a low-energy, all-

purpose collimator and a 35x35-cm field of view. SPECT images were reconstructed by uniformity correction with a 150 million count flood, center-of-rotation correction and low-pass filtering, no attenuation correction, and reconstruction into 1-pixel-thick (5.3-mm) transaxial sections. Oblique angle reorientation and summation produced 3-pixel-thick short-axis left ventricular images. Correction algorithms were applied to the projection images to compensate for motion artifacts.

MRI Protocol

Images were acquired during multiple breath-holds on a 1.5-T whole-body magnet (Signa, General Electric). The pulse sequence used in this study[19] is similar to an inversion-recovery turboFLASH sequence[11] in that pixel intensity is heavily T1-weighted. It was specifically designed to minimize contamination of pixel intensity by both T2 effects, by spoiling magnetization in the xy plane[19] achieved by use of standard radiofrequency phasing algorithms,[20] and T2* effects, by use of a very short TE (2.3 ms). Briefly, within each RR interval, 60 nonselective dummy radiofrequency pulses are transmitted before imaging to drive magnetization to steady state. These are followed immediately by 32 image phase-encoding steps acquired with TR=6.5 ms, TE=2.3 ms, and flip angle=45°. A total of 96 phase-encoding steps per image were acquired, such that each image was completed in three cardiac cycles. K-space lines 1, 4, 7. . . etc; 2, 5, 8. . . etc; and 3, 6, 9. . . etc were acquired during the first, second, and third beats, respectively. Matrix size was 256x96, field of view was 36 cm, and voxel size was 0.9x3.7x10.0 mm.

After scout images were completed, four base-to-apex short-axis cross sections were acquired with prospective ECG gating during each 12-heartbeat breath-hold every 30 seconds for 5 minutes and then at each minute to complete a 10-minute interval begun immediately before contrast administration. The nonionic contrast agent gadoteridol (Squibb, 0.1 mmol/kg) was administered as a bolus by hand injection in a peripheral vein. The entire examination lasted 45 minutes on average, and there were no untoward reactions to gadoteridol.

MRI Data Analysis

Signal-intensity curves over time were generated with the aid of a commercially available software package (GPIX, General Electric). In brief, regions of interest were defined inside the infarcted region represented as a region of hyperenhanced or hypoenhanced signal in the territory perfused by the infarct-related artery determined by coronary angiography. Regions of interest were also defined inside the noninfarcted territory and left ventricular cavity. In patients with hypoenhanced subendocardial zones at the center of the infarcted region, the central region of interest was defined within the central dark zone, while the other regions of interest were placed within regions of increased signal intensity surrounding the central dark zone. The pulse sequence used in these studies produces dark and homogeneous precontrast cardiac images (Fig 1▣). Signal intensity from each image was quantified, and the time-intensity curves generated for each patient (Fig 2▣) were expressed as the percent increase in signal intensity (SI) over baseline precontrast signal intensity as shown below:

Figure 1. A, Left ventricular short-axis cross section from a patient with inferior myocardial infarction. Cardiac signal is suppressed to create a homogeneous image to be enhanced by contrast given
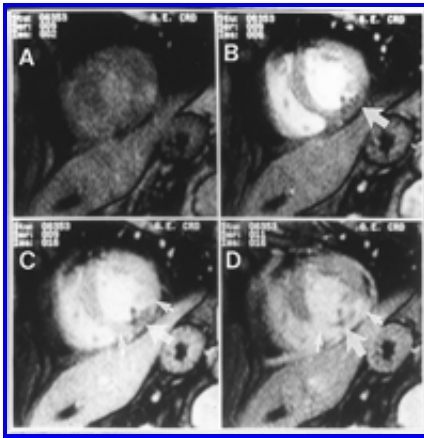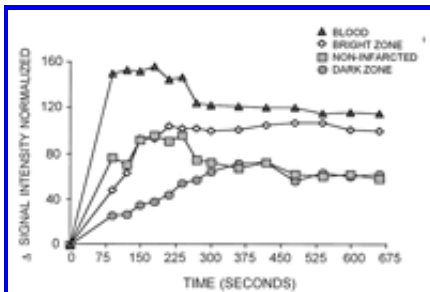
View larger version (180K):
[in this window]
[in a new window]

immediately after baseline images were obtained. B, Both ventricular cavities are highlighted at 50 seconds after contrast, showing also delivery of contrast material to normal myocardium and the delineation of a dark region in the left ventricular inferior wall (arrow). C, Images obtained 160 seconds after contrast administration show hypoenhancement of the central portion of the infarcted zone (large arrow) with hyperenhancement of infarcted regions adjacent to the dark zone (small arrows). D, Late images, obtained 10 minutes after contrast injection, demonstrate hyperenhancement of the infarcted region, which appears as bright as the left ventricular cavity (small arrows). Note also a residual hypoenhanced zone in the center of the infarcted region (large arrow).

View larger version (23K):
[in this window]
[in a new window]

Figure 2. Time-intensity curves from the patient shown in Fig 1⊡ with recent myocardial infarction. Percent increase in signal intensities in blood (▲) and noninfarcted regions (■) is sharp, with slow decay after contrast. Signal intensity in the periphery of the infarcted region (◇) also rises rapidly after contrast but persists at an elevated level, while blood signal intensity is falling. The center of the infarcted region exhibits reduced signal intensity in the first minutes after contrast administration (▪), followed by a progressive rise secondary to delayed contrast penetration into the infarct core.

$$Normalized\ SI\ (\%) = (SI - baseline\ SI / baseline\ SI) \times 100.$$

Normalized time-intensity curves were sampled at three time points (50, 160, and 600 seconds) to describe the time course of myocardial enhancement beyond contrast first pass. The time courses of myocardium-to-blood normalized signal-intensity ratios were analyzed at the same time points. The assessment of the extracellular volume index (ECVi, see "Appendix" for details) was performed in 10 patients, with large areas of signal hyperenhancement uncontaminated by central dark zones. The ECVi was calculated according to the following equation:

$$ECVi = \frac{\Delta SI_{tissue}}{\Delta SI_{blood}} (1 - Hct_{blood})$$

Study Outcomes

The circumferential extent of the sum of hyperenhanced plus hypoenhanced regions was compared with the circumferential extent of the fixed SPECT thallium defect assessed visually from MRI images and thallium scans by two independent investigators. Only the short-axis images obtained at the redistribution phase of the thallium studies, which therefore delineated the fixed thallium defects, were used in this analysis. Both MRI and thallium SPECT abnormalities were quantified at the mid left ventricular wall level and matched by location along the left ventricular long axis. The match was performed by calculating the relative distance of short-axis images from the left ventricular base represented by the mitral valve level. Because only four MRI cross sections were available for seven or eight thallium SPECT cross sections, the thallium short-axis scan that best approximated the MRI short-axis location along the left ventricular long axis was selected for comparison. The average time interval between thallium scintigraphy and MRI was 1 day (range, 0 to 7 days). Thallium scans were interpreted for the presence of fixed or redistribution defects by independent observers who were unaware of the MRI results.

Coronary angiograms were classified by two independent observers in relation to the extent of radiographic contrast penetration downstream from a coronary lesion according to the criteria proposed by the Thrombolysis in Myocardial Infarction (TIMI) study group[9] : grade 0 (no flow), grade 1 (minimal penetration of contrast), grade 2 (delayed flow of contrast), or grade 3 (brisk flow of contrast). Vessels with TIMI grade 0 or 1 were considered occluded and those with grade 2 or 3 were considered patent for statistical analysis purposes. Since 16 of our 22 patients had coronary angioplasty, TIMI flow in the infarct-related artery was assessed both before and after coronary angioplasty. The average time interval between coronary angiography and MRI was 4 days (range, 0 to 10 days).

Echocardiograms were quantified by an independent observer blinded in relation to the MRI and thallium scintigraphic results according to methodology previously described.[21] Global parameters included left ventricular volumes and ejection fraction. The left ventricular wall, defined by endocardial and epicardial contours, was divided into 16 segments by equiangular radial lines placed around the left ventricular cross section.[21] Wall thickness was calculated as the ratio of the segment area to the average of the endocardial and epicardial arc lengths in the short-axis images. Systolic wall thickening was calculated as [(end-systolic minus end-diastolic wall thickness) divided by the end-diastolic wall thickness]x100. Regional dysfunction was characterized as the percent circumferential extent of the sum of segments with systolic wall thickening <5%. ECGs were analyzed by two observers for the presence of Q waves and for infarct location, defined by ECG leads demonstrating Q waves and/or ST-segment changes.

Statistical Analysis

The changes over time of signal intensity obtained from infarcted regions in the MRI scans were compared with the patterns obtained from noninfarcted regions by repeated-measures ANOVA.[22] Differences between specific regions at specific time points were isolated by Bonferroni *t* tests.[22] Moreover, differences in the myocardium-to-blood signal-intensity ratio between patients with open and closed infarct-related arteries were analyzed by profile analysis with repeated-measures ANOVA.[22] Fisher's exact probability tests, Student's *t* tests, and linear regression analyses were also used, as indicated in the text. The data are presented as mean±SEM.

▶ **Results**

Myocardial Infarction and Reperfusion

Therapeutic myocardial reperfusion was attempted in 18 of the 22 patients (see Table 1⊞).
Thrombolytics were used in 17 patients, combined with rescue angioplasty in 4 patients. Direct
angioplasty was performed in 1 patient. Four patients had contraindications to therapeutic
reperfusion and were treated conservatively. Except for the 5 patients who had either rescue
or direct angioplasty, all patients had catheterization at least 48 hours after the onset of myocardial infarction.
Eleven of these 17 patients had percutaneous coronary angioplasty at that time. The average time interval
between coronary angiography and myocardial infarction was 4 days (range, 0 to 11 days).

Myocardial MRI Enhancement Patterns

Three patterns of myocardial signal enhancement on MRI were observed in patients with acute myocardial
infarction (see Figs 1 through 3⊞⊞⊞). In noninfarcted regions, a rapid increase in signal intensity reflecting
adequate tissue contrast delivery is followed by a slower decay (110±17%, 85±12%, and 57±9% at 50, 160,
and 600 seconds after contrast, respectively, Fig 3⊞) caused by the combination of a slowly decaying blood
contrast concentration and the extravasation of contrast material into the interstitial space.[17] [23] [24]

View larger version (19K):
[in this window]
[in a new window]
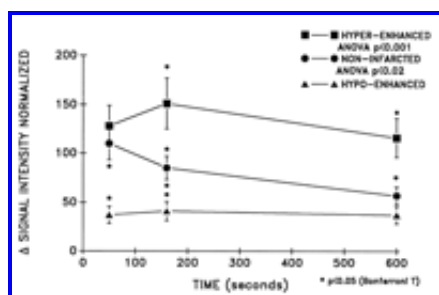
Figure 3. Graph showing percent increase in myocardial signal
intensity (pooled data from all patients) at 50, 160, and 600
seconds after contrast administration. Signal intensity in
noninfarcted regions (●) increases rapidly in the first minute, before
decaying slowly over the next 9 minutes. Infarcted regions (■)
appear hyperenhanced due to rapid signal increase with
persistently high signal intensity. In 10 patients, the center of the
infarcted region (▲) showed low levels of signal intensity in the first
2 to 3 minutes after the contrast bolus.

The second enhancement pattern is characterized by a similarly sharp rise in myocardial signal intensity,
followed, however, by a continued rise in signal intensity over the first 2 minutes and a slower decay than that
observed in normal noninfarcted regions (128±21%, 151±26%, and 116±20% at 50, 160, and 600 seconds,
ANOVA $P<.001$ versus noninfarcted, Fig 3⊞). This enhancement pattern is seen as a "bright area" occupying
the infarcted region and was found in 21 of the 22 patients. One patient had a normal and uniform enhancement
pattern despite a clinical diagnosis of myocardial infarction.

The third pattern, characterized by a slower rate of signal-intensity increase after contrast administration, was
present in 10 patients (37±9%, 41±10%, and 39±9% at 50, 160, and 600 seconds, ANOVA $P<.02$ versus

noninfarcted, Fig 3⊡). It was seen as a "dark zone" involving the subendocardial half of the left ventricular wall at the center of the infarcted region surrounded by regions of hyperenhanced signal intensity. Eventually, protracted contrast penetration into the infarct core produced signal enhancement in the central dark zones, observed in images obtained 5 to 10 minutes after contrast injection (Figs 1⊡ and 2⊡).

Precontrast absolute signal-intensity levels were not different in noninfarcted versus infarcted regions (59.3±8.3 versus 53.2±7.5 for all patients, P=NS). In patients with central dark zones, precontrast signal intensity was similar in noninfarcted (56.4±12.6) and infarcted regions, which later appeared hyperenhanced (52.9±12.6) and hypoenhanced (57.8±15.3, P=NS, ANOVA).

Infarct-Related Artery Patency and Myocardial Enhancement Patterns

Infarct-related artery obstruction at the time of cardiac catheterization was related to the presence of subendocardial dark zones by MRI. When the first angiogram obtained after myocardial infarction was analyzed, coronary arteries with TIMI flow 0 or 1 were associated with a high prevalence (75%) of central dark zones by MRI. The prevalence was lower (20%) in patients with patent coronary arteries but with slow antegrade flow (TIMI 2) and was nil in patients with brisk antegrade flow (TIMI 3, P<.003, Table 2⊡).

View this table: **Table 2.** Presence of Central Hypoenhanced Regions and Patency of the Infarct-
[in this window]   Related Artery
[in a new window]

The analysis was repeated taking into consideration the last angiogram obtained before the MRI study, because 16 patients had coronary angioplasty before MRI (Table 2⊡). Four patients who initially had occluded infarct-related arteries (TIMI 1 or 0) and 3 patients previously in the TIMI 2 group crossed over to the group of patients with patent arteries and brisk antegrade flow (TIMI 3) after angioplasty. The prevalence of patients with central dark zones increased in both groups (83% and 36% in patients with TIMI flow 0 or 1 and TIMI flow 3, respectively), thereby reducing the statistical strength of the association between infarct-related artery obstruction and the presence of hypoenhanced regions by MRI (P<.056, Table 2⊡).

Conversely, the presence of hyperenhanced regions on MRI was not related to patency of the culprit artery by angiography. All patients had either normal or hyperenhanced infarcted regions, indicating that at least the peripheral areas of most human infarcts are perfused by antegrade or collateral blood flow a few days after infarction.

Creatine Phosphokinase, ECG, and Left Ventricular Function

Peak creatine phosphokinase rise was not associated with myocardial perfusion patterns by MRI (1411+309 IU/L for patients with hypoenhanced regions versus 1109+366 IU/L for those without hypoenhanced regions, P=NS). However, the pattern of myocardial perfusion by contrast-enhanced MRI was related to the presence of Q waves on serial ECGs obtained at the time of infarction. Patients with Q-wave infarcts were more likely

(60%) to have hypoenhanced zones than those with non–Q-wave infarcts (14%, *P*<.07, Fisher's exact probability). Ten infarcts were anterior, 10 inferior, and 2 lateral by ECG criteria.

Patients with and without hypoenhanced subendocardial zones within the infarcted regions had similar left ventricular end-diastolic volume (145.3±23.4 versus 130.4±21.6 mL), end-systolic volume (96.1±19.9 versus 68.7±12.2 mL), and ejection fraction (39.7±14.9% versus 46.1±14.9%, respectively, *P*=NS), despite a trend for greater volumes and lower ejection fractions in those with MRI hypoenhanced zones. However, regional dysfunction characterized as a reduction in percent systolic wall thickening <5% was greater in patients with hypoenhanced zones (45.9±8.1%) than those without (22.3±5.6%, *P*<.03, Fig 4▣). The relation was still present, although statistically weaker, when the threshold for dysfunction was set at 0% systolic wall thickening (36.8±10.6% with versus 16.0±2.3% without hypoenhanced zones, *P*<.07, Fig 4▣).

View larger version (20K):
[in this window]
[in a new window]
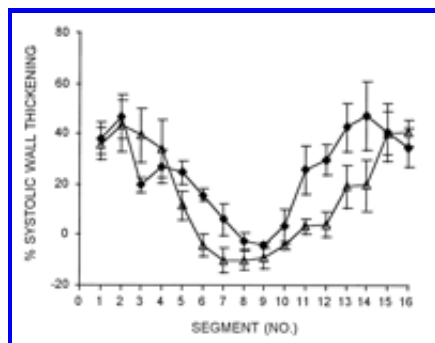
Figure 4. Graph showing percent systolic wall thickening (mean ±SEM) in patients with (△) and without (◆) central hypoenhanced zones for 16 segments distributed around the left ventricular short-axis echocardiograms. Wall-thickening maps from individual patients were averaged by superimposing the center of the segments containing the most severe wall thickening abnormalities. Comparisons between patients with and without central hypoenhanced zones were performed by arbitrary selection of the 5% and 0% thresholds (see "Methods").

Thallium Scintigraphy

Thallium scintigraphy was obtained in 12 patients during exercise and after tracer redistribution 4 hours later. Ten patients had fixed defects corresponding to the acute infarction, but 2 patients had no scintigraphic evidence of infarction despite a rise in creatine phosphokinase. Eight of the 10 patients with fixed thallium defects also had adjacent redistribution defects, suggesting the presence of myocardial ischemia.

The topographic location of fixed thallium defects correlated well with the location of hyperenhanced regions defined by contrast-enhanced MR images (Fig 5▣). In addition, the circumferential extent of the fixed thallium defect in the redistribution scan correlated well with the total extent of the MRI abnormality (the sum of the hypoenhanced plus hyperenhanced regions) in patients with acute myocardial infarction (Fig 6▣).

Figure 5. Top, Left ventricular short-axis single-photon emission computed tomographic thallium scan obtained during tracer redistribution from a patient with left circumflex occlusion who failed thrombolysis but was treated with rescue
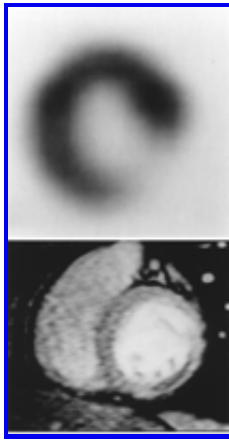
percutaneous transluminal coronary angioplasty within 6 hours of the onset of chest pain. Inferolateral fixed thallium defect is seen 5 days after infarction. Bottom, Left ventricular magnetic resonance imaging (MRI) short-axis image matched by location to the thallium scan shown at top. The central zone of reduced signal enhancement seen in the subendocardial half of the left ventricular wall is surrounded by a region of hyperenhanced signal that corresponds in location and extent to the fixed thallium defect obtained the day before the MRI study.

View larger version (80K):
[in this window]
[in a new window]

View larger version (11K):
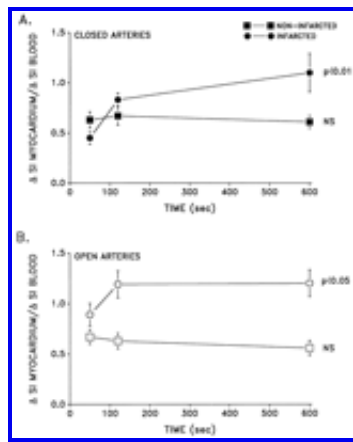[in this window]
[in a new window]
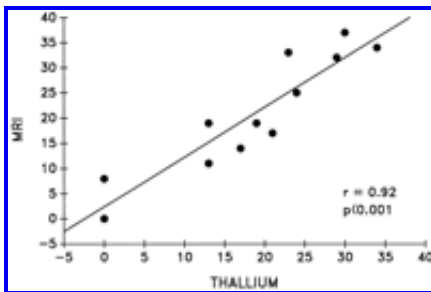
Figure 6. Graph showing circumferential extent of the fixed thallium defect in the short-axis redistribution single-photon emission computed tomographic scan correlates well with the total extent of the magnetic resonance imaging (MRI) perfusion abnormality (the sum of hyperenhanced plus hypoenhanced segments) in patients with myocardial infarction.

Potential Mechanisms of Myocardial Hyperenhancement After Acute Myocardial Infarction

The mechanisms of signal hyperenhancement that characterize infarcted myocardium were explored by study of the time course of signal intensity in myocardium relative to blood after contrast administration. The ratio was not a function of time in noninfarcted regions (Fig 7⊞). However, in the infarcted regions of patients with occluded infarct-related arteries (TIMI 0 or 1), the ratio increased progressively during the first 10 minutes that followed contrast administration, reflecting the contribution of impaired contrast wash-in/washout kinetics as a mechanism of local myocardial hyperenhancement (Fig 7A⊞). Conversely, in patients with open arteries (TIMI 3), the immediate delivery of contrast material to infarcted territory was followed by a further increase in the ratio during the following 2 minutes, reaching a plateau beyond that time point (Fig 7B⊞).

Figure 7. Graphs. A, The myocardium-to-blood signal-intensity ratio in noninfarcted regions (■) of patients with closed infarct-related arteries
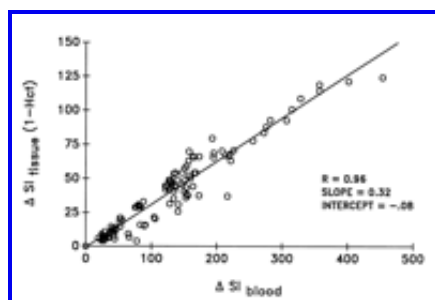
View larger version (18K):
[in this window]
[in a new window]

(TIMI flow 0 or 1, n=6, Table 2◉) remained unchanged after contrast (ANOVA, *P*=NS). However, it increased with time in infarcted regions (◉), suggesting local impairment of contrast wash-in/washout kinetics (ANOVA, *P*<.01). B, In noninfarcted regions of patients with patent arteries (TIMI flow 3, n=14, Table 2◉), the ratio was also unchanged with time (☐). However, in infarcted territory (◯), the ratio increased initially (*P*<.003, ANOVA), reaching a plateau after 160 seconds (time-group interaction *P*<.02 by ANOVA versus patients with closed arteries). This relation suggests a combination of impaired contrast kinetics with an increased contrast volume of distribution in reperfused regions. Δ SI indicates change in signal-intensity ratio.

The upward horizontal displacement of the myocardium-to-blood signal-intensity ratio relative to normal regions suggests the presence of an increased contrast volume of distribution as a mechanism of myocardial hyperenhancement in infarcted territory. This possibility was further explored by plotting myocardial against blood signal intensity for individual images acquired after 2 minutes following contrast administration in 10 patients. Fig 8☑ shows that all data points obtained from noninfarcted regions lie essentially on the same straight line (myocardial SI=-0.8+0.32 blood SI, *r*=.96). The slope of this relation, which characterizes the volume of distribution for the contrast agent in normal myocardium, principally reflects the extracellular compartment volume.[23] [24] The index of extracellular volume, derived from similar relations for each individual patient (see "Appendix"), was greater in infarcted than in noninfarcted myocardium (45.1±2.9% versus 28.4±1.9%, respectively, *P*<.001). These results suggest that the contrast volume of distribution is increased in infarcted regions and may contribute to local myocardial hyperenhancement in infarcted but perfused myocardium.

View larger version (15K):
[in this window]
[in a new window]

Figure 8. Graph showing pooled data from 10 patients with acute myocardial infarction. Δ SI indicates signal-intensity increase in postcontrast images relative to precontrast images but without normalization for baseline signal intensity (see "Methods"). The direct relation between blood (ΔSI_{blood}) and myocardial signal enhancement (ΔSI_{tissue}) in noninfarcted regions is shown (*y*=-0.8+0.32*x*, *r*=.96, *P*<.001). Hct indicates hematocrit.

▶ **Discussion**

Contrast-enhanced MRI allows the identification of two perfusion patterns within human infarcts by comparison with the perfusion pattern of normal, noninfarcted regions. Virtually all patients with clinical myocardial infarction had an area of increased signal intensity within the infarcted region in images obtained 2 to 10 minutes after contrast bolus administration. The only patient who did not have hyperenhancement of the infarcted region had a normal perfusion pattern. In addition, the extent of this area of hyperenhanced signal intensity correlated well with the size of the fixed thallium defect, and its presence was not related to the patency of the infarct-related artery. Therefore, our study, by contrast-enhanced MRI, demonstrates the presence of myocardial blood perfusion within all human infarcts a few days after coronary occlusion. This observation is in agreement with prior studies that used pyrophosphate scintigraphy to demonstrate tracer uptake within infarcted territory after permanent coronary occlusion.[25] [26]

The second pattern consisted of a dark hypoenhanced area located in the subendocardium of the infarcted region within 2 minutes of intravenous contrast bolus administration. These regions were surrounded by areas of increased signal intensity and slowly diminished in size over the course of 5 to 8 minutes after contrast injection. They were associated with closed or nearly closed infarct-related arteries at the time of cardiac catheterization, the presence of Q waves on the ECG, and greater segmental dysfunction by echocardiography. They probably result from protracted contrast penetration with or without hemorrhage, probably caused by severe capillary damage and obstruction at the center of the infarcted region.

The presence of flow inhomogeneity inside infarcted territory is well known from experimental studies using radioactive microspheres after coronary occlusion, which have shown a greater reduction in myocardial blood flow in the subendocardial half of the infarct core.[27] [28] In addition, previous clinical studies have shown flow inhomogeneity inside the infarcted region by contrast echocardiography immediately after direct angioplasty.[9] Our study extends the findings of previous work to demonstrate the persistence of flow inhomogeneity several days after coronary occlusion in association with failure to achieve adequate patency of the infarct-related artery after myocardial infarction and with larger regions of myocardial damage by ECG and echocardiographic criteria. Hypoenhanced zones within the infarcted region were also documented in 2 patients with widely patent infarct-related arteries who failed thrombolysis and underwent successful rescue angioplasty (Fig 5⬚). These central dark regions correlate well with "no-reflow" regions, characterized in previous experimental[27] [28] and clinical[8] [9] studies by the failure to achieve complete myocardial reperfusion after reestablishment of blood supply to the infarcted territory.

Prior experimental studies using spin-echo MRI have demonstrated dark zones surrounded by regions of hyperenhanced signal in occlusive infarcts and basically hyperenhanced signal in infarcted but reperfused myocardium.[13] [14] [15] [16] Our findings correlate well with the results of those animal studies in which patency of the infarct-related artery could be accurately controlled. Spin-echo contrast-enhanced MRI techniques have also shown heterogeneous enhancement patterns within infarcted territory in patients with acute infarction.[29] However, those patterns were difficult to interpret because of the limited temporal resolution of the spin-echo imaging sequence used in those studies. Given the time course of regional enhancement patterns after contrast

bolus administration (Figs 2 and 3), the temporal and topographic features of hypoenhanced zones within the injured territory are best characterized by fast imaging techniques. However, it is theoretically possible to assess the different MRI perfusion patterns documented in our study by conventional or fast spin-echo MRI.
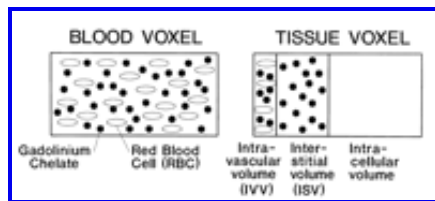
Several previous studies using spin-echo imaging have documented a good correlation between infarct sizes estimated by MRI and by other techniques.[15] [30] [31] [32] Our results are in agreement with those studies that also used the planimetered area encompassed by the MRI signal-intensity abnormality to estimate the extent of ischemic and/or infarcted myocardium. However, because of the trade-off between temporal resolution and number of image planes obtained during a given breath-hold, infarct size was not measured in our study. In addition, in our study, images represent the average of three cardiac cycles with loss of beat-to-beat variations of signal intensity during the contrast bolus first pass through the heart. However, since we did not attempt to extract information on myocardial perfusion from the ascending limb of the time-intensity curves,[11] [33] it is unlikely that the latter factor influenced our results.

Finally, we explored the mechanisms of signal hyperenhancement in infarcted myocardial tissue to gain insight into the pathophysiology of myocardial damage within infarcted regions. Potential mechanisms to explain differences in the time course of the myocardium-to-blood signal-intensity ratio (Fig 7) include (1) impaired myocardial contrast wash-in/washout kinetics, (2) increased contrast volume of distribution, and (3) binding of contrast material to proteins released within injured myocardial tissue.

Our study documents a progressive increase in the infarcted myocardium-to-blood signal-intensity ratio in patients with a totally occluded or nearly occluded infarct-related artery. This finding suggests impairment of contrast wash-in/washout kinetics as a mechanism of myocardial hyperenhancement observed in those patients. Moreover, we estimated the magnitude of extracellular volume expansion in the injured territory of patients with acute myocardial infarction. The almost doubled extracellular space that characterizes human infarcted tissue could represent extracellular edema formation and/or membrane rupture, with consequent diffusion of gadoteridol into the intracellular space. However, although gadoteridol protein binding in normal myocardium is minimal,[34] the possibility of contrast protein binding within infarcted territory cannot be excluded and could potentially contribute to myocardial hyperenhancement in damaged areas after coronary occlusion. Future studies should be directed toward gaining further insight into these mechanisms, which could provide the means to assess myocardial viability after coronary occlusion by MRI.

In conclusion, human myocardial infarcts containing central regions of impaired myocardial blood flow are associated with persistent occlusion of the infarct-related artery and greater regional left ventricular dysfunction. Conversely, infarcts showing uniform contrast hyperenhancement on fast MRI are associated with patent infarct-related arteries and less damage by ECG and echocardiography. Myocardial hyperenhancement by fast MRI results at least in part from impaired contrast kinetics and extracellular space expansion, which may reflect edema formation and/or ruptured cell membranes. Therefore, contrast-enhanced MRI provides unique information on regional myocardial blood perfusion and tissue damage within acute human infarcts.

BLOOD VOXEL   TISSUE VOXEL

Gadolinium   Red Blood   Intra- Inter- Intra-
Chelate   Cell (RBC)   vascular stitial cellular
                          volume volume volume
                          (IVV)   (ISV)

View larger version (21K):
[in this window]
[in a new window]

Figure 9. Hypothetical representation of contrast distribution in blood (left) and myocardial tissue (right) under equilibrium conditions. The extracellular space in this text refers to the sum of the interstitial plus the intravascular volumes minus the volume occupied by red blood cells within the myocardial intravascular space.

▶ Acknowledgments

Increased Contrast Volume of Distribution as a Potential Mechanism of Signal Hyperenhancement in Infarcted Myocardium

The interpretation of the first-pass events that follow bolus administration of contrast are complex.[17] The results of this study, however, in which at best only a single breath-hold occurred under first-pass conditions, are somewhat easier to interpret. By 1 minute after contrast administration, which comprises the vast majority of our data, the contrast agent would be expected to be mixed within the body blood pool. In addition, within myocardial tissue, contrast concentrations between the blood and interstitium would be equilibrated on the basis of known extravasation of this agent[17] and molecules of similar size.[35] Furthermore, the rate of contrast clearance from the blood pool by renal elimination and interstitial space diffusion is slow relative to the time required for equilibration between the myocardial blood pool and the interstitial space.[36] These approximations for noninfarcted regions are supported by our results showing myocardial enhancement as a fixed percentage of blood enhancement (Figs 7 and 8). Thus, our data were acquired at a time when myocardial interstitial contrast concentration equals that of the blood.

Fig 9 shows the hypothetical myocardial distribution of the contrast agent under these conditions. Given the above assumptions, the change in pixel intensity in the tissue (ΔSI_{tissue}) due to the contrast agent can be obtained by

$$\Delta SI_{tissue}=kR[plasma]\{IVV(1-Hct_{tissue})+ISV\}$$

where IVV is intravascular volume, ISV is interstitial volume, k is the slope of pixel intensity versus 1/T1 for the specific pulse sequence used in this study,[19] R is the relaxivity of the contrast agent as further discussed below, [plasma] is plasma contrast concentration, and Hct_{tissue} is tissue hematocrit. Similarly, for blood:

$$\Delta SI_{blood} = kR[plasma](1 - Hct_{blood})$$

If we take the ratio of tissue to blood pixel intensity changes, the constants k, R, and [plasma] cancel:

$$\frac{\Delta SI_{tissue}}{\Delta SI_{blood}} = \frac{IVV(1 - Hct_{tissue}) + ISV}{1 - Hct_{blood}}$$

From this equation, an ECVi can be defined that differs from true extracellular volume in that the volume of red cells within the myocardium is included as cell volume:

$$ECVi = \frac{\Delta SI_{tissue}}{\Delta SI_{blood}}(1 - Hct_{blood})$$

This equation implicitly assumes that (1) myocardial water exchange rates are fast and (2) the imaging pulse sequence results in pixel intensities that are linearly related to 1/T1. These points are individually addressed below.

First, under these nontransient conditions, it is valid to assume that myocardial water exchange rates are fast[17] [23] [24] and that the change in myocardial 1/T1 is linearly related to tissue contrast concentration. Thus, the ratio of the change in 1/T1 of tissue to that of blood is proportional to extracellular volume.

Second, pixel intensities for the pulse sequence used in this study are linearly related to 1/T1 over the range of 0 to 10 s^{-1}.[19] After the first pass of a 0.1 mmol/kg gadoteridol IV bolus, blood and myocardial voxel contrast concentrations would be approximately 0.3 and 0.1 mmol/L, respectively, assuming a myocardial extracellular volume of 30%.[36] For a gadoteridol relaxivity of 4.3 $(mmol/L)^{-1} \cdot s^{-1}$[17] and assuming fast myocardial water exchange,[23] [24] [36] the change in 1/T1 of blood and tissue would be about 1.3 and 0.43 s^{-1}, respectively. These values are well within the range in which image pixel intensity is linearly related to contrast concentration for our pulse sequence,[19] such that the ratio of the change in tissue to blood pixel intensity is proportional to extracellular volume.

Thus, as shown in Fig 8▣, all patients have a similar extracellular volume index for normal myocardium and, within the bounds of the above assumptions, the slope of this line reflects the average extracellular space. In infarcted regions, the above arguments equally apply, and the increased index documented in these hyperenhanced regions (see "Results") reflects, at least in part, a local augmentation in the contrast volume of distribution secondary to an increased extracellular space.

▶ # References

1. Gruppo Italiano per lo Studio della Streptochinasi nell'Infarto Miocardico (GISSI). Effectiveness of intravenous thrombolytic treatment in acute myocardial infarction. *Lancet*. 1986;1:871-874.

2. ISIS 2 (Second International Study of Infarct Survival) Collaborative Group. Randomised trial of intravenous streptokinase, oral aspirin, both, or neither among 17,187 cases of suspected acute myocardial infarction: ISIS-2. *Lancet*. 1988;2:349-360. [Medline] [Order article via Infotrieve]

3. Koren GT, Hasin Y, Appelbaum D, Welber S, Rozenman Y, Lotan C, Mosseri M, Sapoznikov D, Luria MH, Gotsman MS. Prevention of myocardial damage in acute myocardial ischemia by early treatment with intravenous streptokinase. *N Engl J Med*. 1985;313:1384-1389. [Medline] [Order article via Infotrieve]

4. ISIS-3 (Third International Study of Infarct Survival) Collaborative Group. ISIS-3: a randomised comparison of streptokinase vs tissue plasminogen activator vs anistreplase and of aspirin plus heparin vs aspirin alone among 41,229 cases of suspected acute myocardial infarction. *Lancet*. 1992;339:753-770. [Medline] [Order article via Infotrieve]

5. Chesebro JH, Knatterud G, Roberts R, Borer J, Cohen LS, Dalen J, Dodge HT, Francis CK, Hillis D, Ludbrook P, Markis JE, Mueller H, Passamani ER, Powers ER, Rao AK, Robertson T, Ross A, Ryan TJ, Sobel BE, Wellerson J, Williams DO, Waret BL, Braunwald E. Thrombolysis in Myocardial Infarction (TIMI) Trial, phase I: a comparison between intravenous tissue plasminogen activator and intravenous streptokinase. *Circulation*. 1987;76:142-154. [Abstract/Free Full Text]

6. Leung WH, Lau CP. Effects of severity of the residual stenosis of the infarct-related coronary artery on left ventricular dilatation and function after acute myocardial infarction. *J Am Coll Cardiol*. 1992;20:307-313. [Abstract]

7. Gibbons RJ, Holmes DR, Reeder GS, Bailey KR, Hopfenspirger MR, Gersh BJ. Immediate angioplasty compared with the administration of a thrombolytic agent followed by conservative treatment for myocardial infarction. *N Engl J Med*. 1993;328:685-691. [Medline] [Order article via Infotrieve]

8. Schofer J, Montz R, Mathey DG. Scintigraphic evidence of the "no reflow" phenomenon in human beings after coronary thrombolysis. *J Am Coll Cardiol*. 1985;5:593-598. [Abstract]

9. Ito H, Tomooka T, Sakai N, Yu H, Higashino Y, Fujii K, Masuyama T, Kitabatake A, Minamino T. Lack of myocardial perfusion immediately after successful thrombolysis. *Circulation*. 1992;85:1699-1705. [Abstract/Free Full Text]

10. Frahm J, Merboldt KD, Bruhn H, Gyngell ML, Hanicke W, Chien D. A 0.3-second FLASH MRI of the human heart. *Magn Reson Med*. 1990;13:150-157. [Medline] [Order article via Infotrieve]

11. Manning WJ, Atkinson DJ, Grossman W, Paulin S, Edelmann R. First-pass nuclear magnetic resonance imaging studies of patients with coronary artery disease. *J Am Coll Cardiol*. 1991;18:959-965. [Abstract]

12. Van Rugge FP, van der Wall EE, van Dijkman PRM, Louwerenburg HW, de Roos A, Bruschke AVG. Usefulness of ultrafast magnetic resonance imaging in healed myocardial infarction. *Am J Cardiol*.

1992;70:1233-1237. [Medline] [Order article via Infotrieve]

13. Tscholakoff D, Higgins CB, Sechtem U, McNamara MT. Occlusive and reperfused myocardial infarcts: effect of GD-DTPA on ECG-gated MR imaging. *Radiology*. 1986;160:515-519. [Abstract/Free Full Text]

14. Wolfe CL, Moseley ME, Wikstrom MG, Sievers RE, Wendland MR, Dupon JW, Finkbeiner WE, Lipton MJ, Parmley WW, Brasch RC. Assessment of myocardial salvage after ischemia and reperfusion using magnetic resonance imaging and spectroscopy. *Circulation*. 1989;80:969-982. [Abstract/Free Full Text]

15. Schaffer S, Malloy CR, Katz J, Parkey RW, Buja M, Willerson JT, Peshock RM. Gadolinium-DTPA-enhanced nuclear magnetic resonance imaging of reperfused myocardium: identification of the myocardial bed at risk. *J Am Coll Cardiol*. 1988;12:1064-1072. [Abstract]

16. Saeed M, Wagner S, Wendland MF, Derugin N, Finkbeiner WE, Higgins CB. Occlusive and reperfused myocardial infarcts: differentiation with Mn-DPDP-enhanced MR imaging. *Radiology*. 1989;172:59-64. [Abstract/Free Full Text]

17. Judd RM, Atalay MK, Rottman GA, Zerhouni EA. Effects of myocardial water exchange on T1 enhancement during bolus administration of MR contrast agents. *Magn Reson Med*. 1995;33:215-223. [Medline] [Order article via Infotrieve]

18. Clausen M, Bice AN, Civelek AC, Hutchins GM, Wagner HN Jr. Circumferential wall thickness measurements of the human left ventricle: reference data for thallium-201 single-photon emission computed tomography. *Am J Cardiol*. 1986;58:827-831. [Medline] [Order article via Infotrieve]

19. Judd RM, Reeder SB, Atalar E, McVeigh ER, Zerhouni EA. A magnetization-driven gradient echo pulse sequence from the Study of Myocardial Perfusion. *Magn Reson Med*. In press.

20. Zur Y, Wood ML, Neuringer LJ. Spoiling of transverse magnetization in steady state sequences. *Magn Reson Med*. 1991;21:251-263. [Medline] [Order article via Infotrieve]

21. Lima JAC, Becker L, Melin JA, Lima S, Kallman CA, Weisfeldt ML, Weiss JL. Impaired thickening of nonischemic myocardium during acute regional ischemia in the dog. *Circulation*. 1985;71:1048-1059. [Abstract/Free Full Text]

22. Winer BJ. *Statistical Principles in Experimental Design*. 2nd ed. New York, NY: McGraw Hill; 1971:351-359.

23. Burstein D, Taratuta E, Manning WJ. Factors in myocardial `perfusion' imaging with ultrafast MRI and Gd-DTPA administration. *Magn Reson Med*. 1991;20:299-305. [Medline] [Order article via Infotrieve]

24. Tweedle MF, Wedeking P, Telser J, Sotak CH, Chang CA, Kumar K, Wan X, Eaton SM. Dependence of MR signal intensity on Gd tissue concentration over a broad range. *Magn Reson Med*. 1991;22:191-194. [Medline] [Order article via Infotrieve]

25. Buja LM, Parkey RW, Stokely EM, Bonte FJ, Willerson JT. Pathophysiology of technetium-99m stannous pyrophosphate and thallium-201 scintigraphy of acute anterior myocardial infarcts in dogs. *J Clin Invest*. 1976;57:1508-1522.

26. Beller GA, Khaw BA, Haber E, Smith TW. Localization of radiolabeled cardiac myosin-specific antibody in myocardial infarcts: comparison with technetium-99m stannous pyrophosphate. *Circulation.* 1977;55:74-78. [Abstract/Free Full Text]

27. Ambrosio G, Weisman HF, Mannisi JA, Becker LC. Progressive impairment of regional myocardial perfusion after initial restoration of postischemic blood flow. *Circulation.* 1989;80:1846-1861. [Abstract/Free Full Text]

28. Kloner RA, Ganote CE, Jennings RB. The `no-reflow' phenomenon after temporary coronary occlusion in the dog. *J Clin Invest.* 1974;54:1496-1508.

29. De Roos A, van Rossum AC, van der Wall EE, Postema S, Coombos J, Mathejssen NAA, van Dijkman PRM, Visser FC, van Voorthuisen AE. Reperfused and nonreperfused myocardial infarction: diagnostic potential of GD-DTPA-enhanced MR imaging. *Radiology.* 1989;172:717-720. [Abstract/Free Full Text]

30. Goldman MR, Brady TJ, Pykett IL, Burt CT, Buonanno FS, Kistler P, Newhouse JH, Hinshaw WS, Pohost GM. Quantification of experimental myocardial infarction using nuclear magnetic resonance imaging and paramagnetic ion contrast enhancement in excised canine hearts. *Circulation.* 1982;66:1012-1016. [Abstract/Free Full Text]

31. Nishimura T, Yamada Y, Hayashi M, Kozuka T, Nakatani T, Noda H, Takano H. Determination of infarct size of acute myocardial infarction in dogs by magnetic resonance imaging and gadolinium-DTPA: comparison with indium-111 antimyosin imaging. *Am J Physiol Imaging.* 1989;4:82-88.

32. Holman ER, van Jongergen HPW, van Dijkman RM, van der Laarse A, de Roos A, van der Wall E. Comparison of magnetic resonance imaging studies with enzymatic indexes of myocardial necrosis for quantification of myocardial infarct size. *Am J Cardiol.* 1993;71:1036-1040. [Medline] [Order article via Infotrieve]

33. Wilke N, Simm C, Zhang J, Ellermann J, Ya X, Merkle H, Path G, Ludemann H, Bache RJ, Ugurbil K. Contrast-enhanced first pass myocardial perfusion imaging: correlation between myocardial blood flow in dogs at rest and during hyperemia. *Magn Reson Med.* 1993;29:485-497. [Medline] [Order article via Infotrieve]

34. Wedeking P, Sotak CH, Telser J, Kumar K, Chang CA, Tweedle MF. Quantitative dependence of MR signal intensity on tissue concentration of Gd(HP-DO3A) in the nephrectomized rat. *Magn Reson Med.* 1992;10:97-108.

35. Crone C, Levitt DG. Capillary permeability to small solutes. In: Renkin EM, Michel CC, Geiger SR, eds. *Handbook of Physiology.* Bethesda, Md: American Physiological Society; 1984: section 2, vol IV, part II, 411-439.

36. Wolf G. Contrast agents for cardiac MRI. In: Marcus M, Skorton D, Schelbert H, Wolf G, eds. *Cardiac Imaging.* Philadelphia, Pa: WB Saunders Co; 1991:794-810.

This article has been cited by other articles:

Journal of the American College of Cardiology   ▶HOME

N. Mewton, C. Y. Liu, P. Croisille, D. Bluemke, and J. A. C. Lima
Assessment of Myocardial Fibrosis With Cardiovascular Magnetic Resonance
J. Am. Coll. Cardiol., February 22, 2011; 57(8): 891 - 903.
[Abstract] [Full Text] [PDF]

European Heart Journal   ▶HOME

M. Perazzolo Marra, J. A. C. Lima, and S. Iliceto
MRI in acute myocardial infarction
Eur. Heart J., February 1, 2011; 32(3): 284 - 293.
[Abstract] [Full Text] [PDF]

American Journal of Roentgenology   ▶HOME

C. Farrelly, W. Rehwald, M. Salerno, A. Davarpanah, A. N. Keeling, J. T. Jacobson, and J. C. Carr
Improved Detection of Subendocardial Hyperenhancement in Myocardial Infarction Using Dark Blood-Pool Delayed Enhancement MRI
Am. J. Roentgenol., February 1, 2011; 196(2): 339 - 348.
[Abstract] [Full Text] [PDF]

Circulation: Arrhythmia and Electrophysiology   ▶HOME

J. Tian, J. Jeudy, M. F. Smith, A. Jimenez, X. Yin, P. A. Bruce, P. Lei, A. Turgeman, A. Abbo, R. Shekhar, *et al.*
Three-Dimensional Contrast-Enhanced Multidetector CT for Anatomic, Dynamic, and Perfusion Characterization of Abnormal Myocardium To Guide Ventricular Tachycardia Ablations
Circ Arrhythm Electrophysiol, October 1, 2010; 3(5): 496 - 504.
[Abstract] [Full Text] [PDF]

Circulation: Cardiovascular Imaging   ▶HOME

R. A. P. Weir, C. A. Murphy, C. J. Petrie, T. N. Martin, S. Balmain, S. Clements, T. Steedman, G. S. Wagner, H. J. Dargie, and J. J. V. McMurray
Microvascular Obstruction Remains a Portent of Adverse Remodeling in Optimally Treated Patients With Left Ventricular Systolic Dysfunction After Acute Myocardial Infarction
Circ Cardiovasc Imaging, July 1, 2010; 3(4): 360 - 367.
[Abstract] [Full Text] [PDF]

The Journal of Nuclear Medicine   ▶HOME

J. A. Dixon and F. G. Spinale
Pathophysiology of Myocardial Injury and Remodeling: Implications for Molecular Imaging
J. Nucl. Med., May 1, 2010; 51(Supplement_1): 102S - 106S.
[Abstract] [Full Text] [PDF]

Journal of the American College of Cardiology   ▶HOME

S. C. A. M. Bekkers, S. K. Yazdani, R. Virmani, and J. Waltenberger

Microvascular Obstruction: Underlying Pathophysiology and Clinical Diagnosis
J. Am. Coll. Cardiol., April 20, 2010; 55(16): 1649 - 1660.
[Abstract] [Full Text] [PDF]

Radiology   ▸HOME

T. Ibrahim, T. Hackl, S. G. Nekolla, M. Breuer, M. Feldmair, A. Schomig, and M. Schwaiger
Acute Myocardial Infarction: Serial Cardiac MR Imaging Shows a Decrease in Delayed Enhancement of the Myocardium during the 1st Week after Reperfusion
Radiology, January 1, 2010; 254(1): 88 - 97.
[Abstract] [Full Text] [PDF]

American Journal of Roentgenology   ▸HOME

Y. Mikami, H. Sakuma, M. Nagata, M. Ishida, T. Kurita, I. Komuro, and M. Ito
Relation Between Signal Intensity on T2-Weighted MR Images and Presence of Microvascular Obstruction in Patients With Acute Myocardial Infarction
Am. J. Roentgenol., October 1, 2009; 193(4): W321 - W326.
[Abstract] [Full Text] [PDF]

European Respiratory Journal   ▸HOME

L. E. R. McLure and A. J. Peacock
Cardiac magnetic resonance imaging for the assessment of the heart and pulmonary circulation in pulmonary hypertension
Eur. Respir. J., June 1, 2009; 33(6): 1454 - 1466.
[Abstract] [Full Text] [PDF]

Europace   ▸HOME

E. M. Aliot, W. G. Stevenson, J. M. Almendral-Garrote, F. Bogun, C. H. Calkins, E. Delacretaz, P. D. Bella, G. Hindricks, P. Jais, M. E. Josephson, *et al.*
EHRA/HRS Expert Consensus on Catheter Ablation of Ventricular Arrhythmias: Developed in a partnership with the European Heart Rhythm Association (EHRA), a Registered Branch of the European Society of Cardiology (ESC), and the Heart Rhythm Society (HRS); in collaboration with the American College of Cardiology (ACC) and the American Heart Association (AHA)
Europace, June 1, 2009; 11(6): 771 - 817.
[Full Text] [PDF]

Circulation: Arrhythmia and Electrophysiology   ▸HOME

S. Nazarian, D. A. Bluemke, and H. R. Halperin
Applications of Cardiac Magnetic Resonance in Electrophysiology
Circ Arrhythm Electrophysiol, February 1, 2009; 2(1): 63 - 71.
[Full Text] [PDF]

Radiology   ▸HOME

R. Nijveldt, M. B. M. Hofman, A. Hirsch, A. M. Beek, V. A. W. M. Umans, P.

R. Algra, J. J. Piek, and A. C. van Rossum
Assessment of Microvascular Obstruction and Prediction of Short-term Remodeling after Acute Myocardial Infarction: Cardiac MR Imaging Study
Radiology, February 1, 2009; 250(2): 363 - 370.
[Abstract] [Full Text] [PDF]

> HOME

M.-Y. M. Su, B.-C. Lee, Y.-W. Wu, H.-Y. Yu, W.-C. Chu, and W.-Y. I. Tseng
Perfusion of Residual Viable Myocardium in Nontransmural Infarct Zone after Intervention: MR Quantitative Myocardial Blood Flow Measurement
Radiology, December 1, 2008; 249(3): 820 - 828.
[Abstract] [Full Text] [PDF]

THE BRITISH JOURNAL OF RADIOLOGY   > HOME

T BRAHMBHATT, P HARI, M CINQUEGRANI, N KUMAR, R KOMOROWSKI, and R Q MIGRINO
Delayed enhancement on cardiac MRI in a patient with multiple myeloma without amyloidosis
Br. J. Radiol., November 1, 2008; 81(971): e272 - e275.
[Abstract] [Full Text] [PDF]

EUROPEAN JOURNAL OF CARDIO-THORACIC SURGERY   > HOME

F. B. Sozzi, L. Iacuzio, F. Civaia, and V. Dor
Contrast-enhanced magnetic resonance imaging guided decision making after primary percutaneous coronary intervention for acute ST-elevation inferior myocardial infarction.
Eur. J. Cardiothorac. Surg., August 1, 2008; 34(2): 463 - 465.
[Abstract] [Full Text] [PDF]
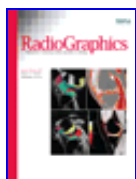

Journal of the American College of Cardiology   > HOME

R. Nijveldt, A. M. Beek, A. Hirsch, M. G. Stoel, M. B.M. Hofman, V. A.W.M. Umans, P. R. Algra, J. W.R. Twisk, and A. C. van Rossum
Functional recovery after acute myocardial infarction comparison between angiography, electrocardiography, and cardiovascular magnetic resonance measures of microvascular injury.
J. Am. Coll. Cardiol., July 15, 2008; 52(3): 181 - 189.
[Abstract] [Full Text] [PDF]

RadioGraphics   > HOME

F. Saremi, J. D. Grizzard, and R. J. Kim
Optimizing Cardiac MR Imaging: Practical Remedies for Artifacts1
RadioGraphics, July 1, 2008; 28(4): 1161 - 1187.
[Abstract] [Full Text] [PDF]

Journal of the American College of Cardiology   > HOME

A. Hirsch, R. Nijveldt, J. D.E. Haeck, A. M. Beek, K. T. Koch, J. P.S. Henriques, R. J. van der Schaaf, M. M. Vis, J. Baan Jr, R. J. de Winter, *et al.*
Relation between the assessment of microvascular injury by cardiovascular magnetic resonance and coronary Doppler flow

velocity measurements in patients with acute anterior wall
myocardial infarction.
J. Am. Coll. Cardiol., June 10, 2008; 51(23): 2230 - 2238.
[Abstract] [Full Text] [PDF]

Journal of the American College of Cardiology   ▸HOME

C. E. Rochitte
**Microvascular obstruction the final frontier for a complete
myocardial reperfusion.**
J. Am. Coll. Cardiol., June 10, 2008; 51(23): 2239 - 2240.
[Full Text] [PDF]

HEART ONLINE and EDUCATION IN HEART   ▸HOME

E Wu, J T Ortiz, P Tejedor, D C Lee, C Bucciarelli-Ducci, P Kansal, J C Carr,
T A Holly, D Lloyd-Jones, F J Klocke, *et al.*
**Infarct size by contrast enhanced cardiac magnetic resonance is a
stronger predictor of outcomes than left ventricular ejection fraction
or end-systolic volume index: prospective cohort study**
Heart, June 1, 2008; 94(6): 730 - 736.
[Abstract] [Full Text] [PDF]

Journal of the American College of Cardiology   ▸HOME

M. G. Friedrich, H. Abdel-Aty, A. Taylor, J. Schulz-Menger, D. Messroghli,
and R. Dietz
**The salvaged area at risk in reperfused acute myocardial infarction
as visualized by cardiovascular magnetic resonance.**
J. Am. Coll. Cardiol., April 22, 2008; 51(16): 1581 - 1587.
[Abstract] [Full Text] [PDF]

Radiology   ▸HOME

K. Nieman, M. D. Shapiro, M. Ferencik, C. H. Nomura, S. Abbara, U.
Hoffmann, H. K. Gold, I.-K. Jang, T. J. Brady, and R. C. Cury
**Reperfused Myocardial Infarction: Contrast-enhanced 64-Section CT
in Comparison to MR Imaging**
Radiology, April 1, 2008; 247(1): 49 - 56.
[Abstract] [Full Text] [PDF]

Journal of the American College of Cardiology: Cardiovascular Imaging ▸HOME

T. Dickfeld, P. Lei, V. Dilsizian, J. Jeudy, J. Dong, A. Voudouris, R. Peters,
M. Saba, R. Shekhar, and S. Shorofsky
**Integration of three-dimensional scar maps for ventricular
tachycardia ablation with positron emission tomography-computed
tomography.**
J. Am. Coll. Cardiol. Img., January 1, 2008; 1(1): 73 - 82.
[Abstract] [Full Text] [PDF]

HEART ONLINE and EDUCATION IN HEART   ▸HOME

J. F Younger, S. Plein, J. Barth, J. P Ridgway, S. G Ball, and J. P
Greenwood
**Troponin-I concentration 72 h after myocardial infarction correlates
with infarct size and presence of microvascular obstruction**
Heart, December 1, 2007; 93(12): 1547 - 1551.

Radiology   ▶ HOME

V. R. S. Fernandes, K. C. Wu, B. D. Rosen, A. Schmidt, A. C. Lardo, N.
Osman, H. R. Halperin, G. Tomaselli, R. Berger, D. A. Bluemke, *et al.*
**Enhanced Infarct Border Zone Function and Altered Mechanical
Activation Predict Inducibility of Monomorphic Ventricular
Tachycardia in Patients with Ischemic Cardiomyopathy**
Radiology, December 1, 2007; 245(3): 712 - 719.

Journal of the American College of Cardiology   ▶ HOME

T. Vartdal, H. Brunvand, E. Pettersen, H.-J. Smith, E. Lyseggen, T. Helle-
Valle, H. Skulstad, H. Ihlen, and T. Edvardsen
**Early Prediction of Infarct Size by Strain Doppler Echocardiography
After Coronary Reperfusion**
J. Am. Coll. Cardiol., April 24, 2007; 49(16): 1715 - 1721.

The Journal of THORACIC AND CARDIOVASCULAR SURGERY   ▶ HOME

M. A. Harris, T. R. Johnson, P. M. Weinberg, and M. A. Fogel
**Delayed-enhancement cardiovascular magnetic resonance identifies
fibrous tissue in children after surgery for congenital heart disease**
J. Thorac. Cardiovasc. Surg., March 1, 2007; 133(3): 676 - 681.

Radiology   ▶ HOME

J. P. Finn, K. Nael, V. Deshpande, O. Ratib, and G. Laub
Cardiac MR Imaging: State of the Technology.
Radiology, November 1, 2006; 241(2): 338 - 354.

Radiology   ▶ HOME

G. L. Raff, W. W. O'Neill, R. E. Gentry, A. Dulli, K. G. Bis, A. N. Shetty, and
J. A. Goldstein
**Microvascular Obstruction and Myocardial Function after Acute
Myocardial Infarction: Assessment by Using Contrast-enhanced Cine
MR Imaging.**
Radiology, August 1, 2006; 240(2): 529 - 536.

Circulation   ▶ HOME

B. L. Gerber, B. Belge, G. J. Legros, P. Lim, A. Poncelet, A. Pasquet, G.
Gisellu, E. Coche, and J.-L. J. Vanoverschelde
**Characterization of Acute and Chronic Myocardial Infarcts by
Multidetector Computed Tomography: Comparison With Contrast-
Enhanced Magnetic Resonance**
Circulation, February 14, 2006; 113(6): 823 - 833.

Circulation   ▶ HOME

A. C. Lardo, M. A.S. Cordeiro, C. Silva, L. C. Amado, R. T. George, A. P. Saliaris, K. H. Schuleri, V. R. Fernandes, M. Zviman, S. Nazarian, *et al.*
Contrast-Enhanced Multidetector Computed Tomography Viability Imaging After Myocardial Infarction: Characterization of Myocyte Death, Microvascular Obstruction, and Chronic Scar
Circulation, January 24, 2006; 113(3): 394 - 404.
[Abstract] [Full Text] [PDF]

Journal of the American College of Cardiology ▸HOME

T. Dickfeld, R. Kato, M. Zviman, S. Lai, G. Meininger, A. C. Lardo, A. Roguin, D. Blumke, R. Berger, H. Calkins, *et al.*
Characterization of Radiofrequency Ablation Lesions With Gadolinium-Enhanced Cardiovascular Magnetic Resonance Imaging
J. Am. Coll. Cardiol., January 17, 2006; 47(2): 370 - 378.
[Abstract] [Full Text] [PDF]

Circulation ▸HOME

S. Nazarian, D. A. Bluemke, A. C. Lardo, M. M. Zviman, S. P. Watkins, T. L. Dickfeld, G. R. Meininger, A. Roguin, H. Calkins, G. F. Tomaselli, *et al.*
Magnetic Resonance Assessment of the Substrate for Inducible Ventricular Tachycardia in Nonischemic Cardiomyopathy
Circulation, November 1, 2005; 112(18): 2821 - 2825.
[Abstract] [Full Text] [PDF]

Journal of the American College of Cardiology ▸HOME

G. Tarantini, L. Cacciavillani, F. Corbetti, A. Ramondo, M. P. Marra, E. Bacchiega, M. Napodano, C. Bilato, R. Razzolini, and S. Iliceto
Duration of Ischemia Is a Major Determinant of Transmurality and Severe Microvascular Obstruction After Primary Angioplasty: A Study Performed With Contrast-Enhanced Magnetic Resonance
J. Am. Coll. Cardiol., October 4, 2005; 46(7): 1229 - 1235.
[Abstract] [Full Text] [PDF]

European Heart Journal ▸HOME

K. G. Blyth, B. A. Groenning, T. N. Martin, J. E. Foster, P. B. Mark, H. J. Dargie, and A. J. Peacock
Contrast enhanced-cardiovascular magnetic resonance imaging in patients with pulmonary hypertension
Eur. Heart J., October 1, 2005; 26(19): 1993 - 1999.
[Abstract] [Full Text] [PDF]

HEART ONLINE and EDUCATION IN HEART ▸HOME

H Bulow, C Klein, I Kuehn, R Hollweck, S G Nekolla, K Schreiber, F Haas, J Bohm, B Schnackenburg, R Lange, *et al.*
Cardiac magnetic resonance imaging: long term reproducibility of the late enhancement signal in patients with chronic coronary artery disease
Heart, September 1, 2005; 91(9): 1158 - 1163.
[Abstract] [Full Text] [PDF]

Journal of the American College of Cardiology ▸HOME

M. J. Budoff, M. C. Cohen, M. J. Garcia, J. McB. Hodgson, W. G. Hundley, J. A.C. Lima, W. J. Manning, G. M. Pohost, P. M. Raggi, G. P. Rodgers, *et al.*
ACCF/AHA Clinical Competence Statement on Cardiac Imaging With Computed Tomography and Magnetic Resonance: A Report of the American College of Cardiology Foundation/American Heart Association/American College of Physicians Task Force on Clinical Competence and Training
J. Am. Coll. Cardiol., July 19, 2005; 46(2): 383 - 402.
[Full Text] [PDF]

Circulation   ›HOME

V. Fuster and R. J. Kim
Frontiers in Cardiovascular Magnetic Resonance
Circulation, July 5, 2005; 112(1): 135 - 144.
[Full Text] [PDF]

Radiology   ›HOME

T. K. F. Foo, V. B. Ho, M. Saranathan, L.-q. Cheng, H. Sakuma, D. L. Kraitchman, K. C. Wu, and D. A. Bluemke
Feasibility of Integrating High-Spatial-Resolution 3D Breath-hold Coronary MR Angiography with Myocardial Perfusion and Viability Examinations
Radiology, June 1, 2005; 235(3): 1025 - 1030.
[Abstract] [Full Text] [PDF]

The Journal of Nuclear Medicine   ›HOME

P. J. Slomka, D. Fieno, L. Thomson, J. D. Friedman, S. W. Hayes, G. Germano, and D. S. Berman
Automatic Detection and Size Quantification of Infarcts by Myocardial Perfusion SPECT: Clinical Validation by Delayed-Enhancement MRI
J. Nucl. Med., May 1, 2005; 46(5): 728 - 735.
[Abstract] [Full Text] [PDF]

European Heart Journal   ›HOME

V. Hombach, O. Grebe, N. Merkle, S. Waldenmaier, M. Hoher, M. Kochs, J. Wohrle, and H. A. Kestler
Sequelae of acute myocardial infarction regarding cardiac structure and function and their prognostic significance as assessed by magnetic resonance imaging
Eur. Heart J., March 2, 2005; 26(6): 549 - 557.
[Abstract] [Full Text] [PDF]

Journal of the American College of Cardiology   ›HOME

T. Ibrahim, S. G. Nekolla, M. Hornke, H. P. Bulow, J. Dirschinger, A. Schomig, and M. Schwaiger
Quantitative measurement of infarct size by contrast-enhanced magnetic resonance imaging early after acute myocardial infarction: Comparison with single-photon emission tomography using Tc99m-sestamibi
J. Am. Coll. Cardiol., February 15, 2005; 45(4): 544 - 552.
[Abstract] [Full Text] [PDF]

Circulation

R. Y. Kwong and R. H. Falk
Cardiovascular Magnetic Resonance in Cardiac Amyloidosis
Circulation, January 18, 2005; 111(2): 122 - 124.
[Full Text] [PDF]

> HOME

Journal of the American College of Cardiology

L. C. Amado, B. L. Gerber, S. N. Gupta, D. W. Rettmann, G. Szarf, R. Schock, K. Nasir, D. L. Kraitchman, and J. A.C. Lima
Accurate and objective infarct sizing by contrast-enhanced magnetic resonance imaging in a canine myocardial infarction model
J. Am. Coll. Cardiol., December 21, 2004; 44(12): 2383 - 2389.
[Abstract] [Full Text] [PDF]

> HOME

Radiology

J. Garot, J. A. C. Lima, B. L. Gerber, S. Sampath, K. C. Wu, D. A. Bluemke, J. L. Prince, and N. F. Osman
Spatially Resolved Imaging of Myocardial Function with Strain-encoded MR: Comparison with Delayed Contrast-enhanced MR Imaging after Myocardial Infarction
Radiology, November 1, 2004; 233(2): 596 - 602.
[Abstract] [Full Text] [PDF]

> HOME

Journal of the American College of Cardiology

J. A.C. Lima and M. Y. Desai
Cardiovascular magnetic resonance imaging: Current and emerging applications
J. Am. Coll. Cardiol., September 15, 2004; 44(6): 1164 - 1171.
[Abstract] [Full Text] [PDF]

> HOME

Radiology

R. R. Edelman
Contrast-enhanced MR Imaging of the Heart: Overview of the Literature
Radiology, September 1, 2004; 232(3): 653 - 668.
[Abstract] [Full Text] [PDF]

> HOME

European Heart Journal

C. F. Azevedo, L. C. Amado, D. L. Kraitchman, B. L. Gerber, N. F. Osman, C. E. Rochitte, T. Edvardsen, and J. A.C. Lima
Persistent diastolic dysfunction despite complete systolic functional recovery after reperfused acute myocardial infarction demonstrated by tagged magnetic resonance imaging
Eur. Heart J., August 2, 2004; 25(16): 1419 - 1427.
[Abstract] [Full Text] [PDF]

> HOME

European Journal of Heart Failure

A. Cochet, M. Zeller, Y. Cottin, C. Robert-Valla, A. Lalande, I. L'Huilllier, A. Comte, P. M. Walker, J. Desgres, J.-E. Wolf, *et al.*
The extent of myocardial damage assessed by contrast-enhanced MRI is a major determinant of N-BNP concentration after myocardial infarction

> HOME

Eur J Heart Fail, August 1, 2004; 6(5): 555 - 560.
[Abstract] [Full Text] [PDF]

Radiology   ▸HOME

R. Muthupillai, S. D. Flamm, J. M. Wilson, R. I. Pettigrew, and W. T. Dixon
Acute Myocardial Infarction: Tissue Characterization with T1{rho}-weighted MR Imaging--Initial Experience
Radiology, August 1, 2004; 232(2): 606 - 610.
[Abstract] [Full Text] [PDF]

Radiology   ▸HOME

G. K. Lund, A. Stork, M. Saeed, M. P. Bansmann, J. H. Gerken, V. Muller, J. Mester, C. B. Higgins, G. Adam, and T. Meinertz
Acute Myocardial Infarction: Evaluation with First-Pass Enhancement and Delayed Enhancement MR Imaging Compared with 201Tl SPECT Imaging
Radiology, July 1, 2004; 232(1): 49 - 57.
[Abstract] [Full Text] [PDF]

Circulation   ▸HOME

H. Abdel-Aty, A. Zagrosek, J. Schulz-Menger, A. J. Taylor, D. Messroghli, A. Kumar, M. Gross, R. Dietz, and M. G. Friedrich
Delayed Enhancement and T2-Weighted Cardiovascular Magnetic Resonance Imaging Differentiate Acute From Chronic Myocardial Infarction
Circulation, May 25, 2004; 109(20): 2411 - 2416.
[Abstract] [Full Text] [PDF]

European Heart Journal   ▸HOME

S.R. Underwood, J. J Bax, J. v. Dahl, M. Y Henein, A. C van Rossum, E. R Schwarz, J.-L. Vanoverschelde, E. E.v. d. Wall, and W. Wijns
Imaging techniques for the assessment of myocardial hibernation: Report of a Study Group of the European Society of Cardiology
Eur. Heart J., May 2, 2004; 25(10): 815 - 836.
[Abstract] [Full Text] [PDF]

Journal of the American College of Cardiology   ▸HOME

L. C. Amado, D. L. Kraitchman, B. L. Gerber, E. Castillo, R. C. Boston, J. Grayzel, and J. A. C. Lima
Reduction of "no-reflow" phenomenon by intra-aortic balloon counterpulsation in a randomized magnetic resonance imaging experimental study
J. Am. Coll. Cardiol., April 7, 2004; 43(7): 1291 - 1298.
[Abstract] [Full Text] [PDF]

Circulation   ▸HOME

K. Shan, G. Constantine, M. Sivananthan, and S. D. Flamm
Role of Cardiac Magnetic Resonance Imaging in the Assessment of Myocardial Viability
Circulation, March 23, 2004; 109(11): 1328 - 1334.
[Full Text] [PDF]

Radiology   ▶HOME

T. K. F. Foo, D. W. Stanley, E. Castillo, C. E. Rochitte, Y. Wang, J. A. C.
Lima, D. A. Bluemke, and K. C. Wu
**Myocardial Viability: Breath-hold 3D MR Imaging of Delayed
Hyperenhancement with Variable Sampling in Time**
Radiology, March 1, 2004; 230(3): 845 - 851.
[Abstract] [Full Text] [PDF]

Circulation Research   ▶HOME

K. C. Wu and J. A.C. Lima
**Noninvasive Imaging of Myocardial Viability: Current Techniques and
Future Developments**
Circ. Res., December 12, 2003; 93(12): 1146 - 1158.
[Abstract] [Full Text] [PDF]

Journal of the American College of Cardiology   ▶HOME

A. M. Beek, H. P. Kuhl, O. Bondarenko, J. W. R. Twisk, M. B. M. Hofman,
W. G. van Dockum, C. A. Visser, and A. C. van Rossum
**Delayed contrast-enhanced magnetic resonance imaging for the
prediction of regional functional improvement after acute
myocardial infarction**
J. Am. Coll. Cardiol., September 3, 2003; 42(5): 895 - 901.
[Abstract] [Full Text] [PDF]

Journal of the American College of Cardiology   ▶HOME

J. A. C. Lima
**Myocardial viability assessment by contrast-enhanced magnetic
resonance imaging**
J. Am. Coll. Cardiol., September 3, 2003; 42(5): 902 - 904.
[Full Text] [PDF]

Journal of the American College of Cardiology   ▶HOME

R. J. Kim and R. M. Judd
**Gadolinium-Enhancedmagnetic resonance imagingin hypertrophic
cardiomyopathy: In vivo imaging of the pathologic substrate for
premature cardiac death?**
J. Am. Coll. Cardiol., May 7, 2003; 41(9): 1568 - 1572.
[Full Text] [PDF]

Radiology   ▶HOME

S. Flacke, J. S. Allen, J. M. Chia, J. H. Wible, M. P. Periasamy, M. D.
Adams, I. K. Adzamli, and C. H. Lorenz
**Characterization of Viable and Nonviable Myocardium at MR
Imaging: Comparison of Gadolinium-based Extracellular and Blood
Pool Contrast Materials versus Manganese-based Contrast Materials
in a Rat Myocardial Infarction Model**
Radiology, March 1, 2003; 226(3): 731 - 738.
[Abstract] [Full Text] [PDF]

Radiology   ▶HOME

S. S. Lee, H. W. Goo, S. B. Park, C. H. Lim, G. Gong, J. B. Seo, and T.-H.
Lim

MR Imaging of Reperfused Myocardial Infarction: Comparison of Necrosis-Specific and Intravascular Contrast Agents in a Cat Model
Radiology, March 1, 2003; 226(3): 739 - 747.
[Abstract] [Full Text] [PDF]

CHEST   ▸HOME

J.-P. Laissy, B. Messin, O. Varenne, B. Iung, D. Karila-Cohen, E. Schouman-Claeys, and P. G. Steg
MRI of Acute Myocarditis: A Comprehensive Approach Based on Various Imaging Sequences
Chest, November 1, 2002; 122(5): 1638 - 1648.
[Abstract] [Full Text] [PDF]

Circulation   ▸HOME

B. L. Gerber, J. Garot, D. A. Bluemke, K. C. Wu, and J. A.C. Lima
Accuracy of Contrast-Enhanced Magnetic Resonance Imaging in Predicting Improvement of Regional Myocardial Function in Patients After Acute Myocardial Infarction
Circulation, August 27, 2002; 106(9): 1083 - 1089.
[Abstract] [Full Text] [PDF]

Circulation   ▸HOME

E. C. Perin, G. V. Silva, R. Sarmento-Leite, A. L.S. Sousa, M. Howell, R. Muthupillai, B. Lambert, W. K. Vaughn, and S. D. Flamm
Assessing Myocardial Viability and Infarct Transmurality With Left Ventricular Electromechanical Mapping in Patients With Stable Coronary Artery Disease: Validation by Delayed-Enhancement Magnetic Resonance Imaging
Circulation, August 20, 2002; 106(8): 957 - 961.
[Abstract] [Full Text] [PDF]

American Journal of Roentgenology   ▸HOME

B. Kumbasar, K. C. Wu, I. R. Kamel, J. A. C. Lima, and D. A. Bluemke
Left Ventricular True Aneurysm: Diagnosis of Myocardial Viability Shown on MR Imaging
Am. J. Roentgenol., August 1, 2002; 179(2): 472 - 474.
[Full Text] [PDF]

European Heart Journal   ▸HOME

H. Mahrholdt, A. Wagner, R.M. Judd, and U. Sechtem
Assessment of myocardial viability by cardiovascular magnetic resonance imaging
Eur. Heart J., April 2, 2002; 23(8): 602 - 619.
[Full Text] [PDF]

Radiology   ▸HOME

J. J. W. Sandstede, T. Pabst, M. Beer, C. Lipke, K. Baurle, F. Butter, K. Harre, W. Kenn, W. Voelker, S. Neubauer, *et al.*
Assessment of Myocardial Infarction in Humans with 23Na MR Imaging: Comparison with Cine MR Imaging and Delayed Contrast Enhancement
Radiology, October 1, 2001; 221(1): 222 - 228.

Circulation ▸ HOME

B. L. Gerber, C. E. Rochitte, D. A. Bluemke, J. A. Melin, P. Crosille, L. C. Becker, and J. A.C. Lima
Relation Between Gd-DTPA Contrast Enhancement and Regional Inotropic Response in the Periphery and Center of Myocardial Infarction
Circulation, August 28, 2001; 104(9): 998 - 1004.
[Abstract] [Full Text] [PDF]

Journal of the American College of Cardiology ▸ HOME

S. B. Yeon, N. Reichek, B. A. Tallant, J. A. C. Lima, L. P. Calhoun, N. R. Clark, E. A. Hoffman, K. K. L. Ho, and L. Axel
Validation of in vivo myocardial strain measurement by magnetic resonance tagging with sonomicrometry
J. Am. Coll. Cardiol., August 1, 2001; 38(2): 555 - 561.
[Abstract] [Full Text] [PDF]

RadioGraphics ▸ HOME

S. B. Reeder, Y. P. Du, J. A. C. Lima, and D. A. Bluemke
Advanced Cardiac MR Imaging of Ischemic Heart Disease
RadioGraphics, July 1, 2001; 21(4): 1047 - 1074.
[Abstract] [Full Text] [PDF]

HEART ONLINE and EDUCATION IN HEART ▸ HOME

J C Nilsson, G Nielsen, B A Groenning, T Fritz-Hansen, L Sondergaard, G B Jensen, and H B W Larsson
Sustained postinfarction myocardial oedema in humans visualised by magnetic resonance imaging
Heart, June 1, 2001; 85(6): 639 - 642.
[Abstract] [Full Text]

European Heart Journal Supplements ▸ HOME

U. Sechtem
Imaging myocardial area at risk and final infarct size
Eur. Heart J. Suppl., June 1, 2001; 3(suppl_C): C36 - C46.
[PDF]

Experimental Biology & Medicine ▸ HOME

M. Saeed
New Concepts in Characterization of Ischemically Injured Myocardium by MRI
Exp Biol Med, May 1, 2001; 226(5): 367 - 376.
[Abstract] [Full Text] [PDF]

Radiology ▸ HOME

S. J. Flacke, S. E. Fischer, and C. H. Lorenz
Measurement of the Gadopentetate Dimeglumine Partition Coefficient in Human Myocardium in Vivo: Normal Distribution and Elevation in Acute and Chronic Infarction

Radiology, March 1, 2001; 218(3): 703 - 710.
[Abstract] [Full Text]

Circulation   ▶HOME

M. Saeed, G. Lund, M. F. Wendland, J. Bremerich, H.-J. Weinmann, and C. B. Higgins
Magnetic Resonance Characterization of the Peri-Infarction Zone of Reperfused Myocardial Infarction With Necrosis-Specific and Extracellular Nonspecific Contrast Media
Circulation, February 13, 2001; 103(6): 871 - 876.
[Abstract] [Full Text] [PDF]

Am. J. Physiol: Heart and Circulatory Physiology   ▶HOME

T. Wolf, L. Gepstein, G. Hayam, A. Zaretzky, R. Shofty, D. Kirshenbaum, G. Uretzky, U. Oron, and S. A. Ben-Haim
Three-dimensional endocardial impedance mapping: a new approach for myocardial infarction assessment
Am J Physiol Heart Circ Physiol, January 1, 2001; 280(1): H179 - H188.
[Abstract] [Full Text] [PDF]

Radiology   ▶HOME

O. P. Simonetti, R. J. Kim, D. S. Fieno, H. B. Hillenbrand, E. Wu, J. M. Bundy, J. P. Finn, and R. M. Judd
An Improved MR Imaging Technique for the Visualization of Myocardial Infarction
Radiology, January 1, 2001; 218(1): 215 - 223.
[Abstract] [Full Text]

Radiology   ▶HOME

K. Lauerma, P. Niemi, H. Hanninen, T. Janatuinen, L.-M. Voipio-Pulkki, J. Knuuti, L. Toivonen, T. Makela, M. A. Makijarvi, and H. J. Aronen
Multimodality MR Imaging Assessment of Myocardial Viability: Combination of First-Pass and Late Contrast Enhancement to Wall Motion Dynamics and Comparison with FDG PET-Initial Experience
Radiology, December 1, 2000; 217(3): 729 - 736.
[Abstract] [Full Text]

JACC **Journal of the American College of Cardiology**   ▶HOME

C. M. Kramer, W. J. Rogers Jr., S. Mankad, T. M. Theobald, D. L. Pakstis, and Y.-L. Hu
Contractile reserve and contrast uptake pattern by magnetic resonance imaging and functional recovery after reperfused myocardial infarction
J. Am. Coll. Cardiol., November 15, 2000; 36(6): 1835 - 1840.
[Abstract] [Full Text] [PDF]

Circulation Research   ▶HOME

C. E. Rochitte, R. J. Kim, H. B. Hillenbrand, E.-I. Chen, and J. A. C. Lima
Microvascular Integrity and the Time Course of Myocardial Sodium Accumulation After Acute Infarction

Circ. Res., October 13, 2000; 87(8): 648 - 655.
[Abstract] [Full Text] [PDF]

European Journal of Heart Failure   ▶HOME

K. Rajappan, N. G. Bellenger, L. Anderson, and D. J. Pennell
The role of cardiovascular magnetic resonance in heart failure
Eur J Heart Fail, September 1, 2000; 2(3): 241 - 252.
[Abstract] [Full Text] [PDF]

Circulation   ▶HOME

B. L. Gerber, C. E. Rochitte, J. A. Melin, E. R. McVeigh, D. A. Bluemke, K.
C. Wu, L. C. Becker, and J. A. C. Lima
**Microvascular Obstruction and Left Ventricular Remodeling Early
After Acute Myocardial Infarction**
Circulation, June 13, 2000; 101(23): 2734 - 2741.
[Abstract] [Full Text] [PDF]

American Journal of Roentgenology   ▶HOME

J. J. W. Sandstede, C. Lipke, M. Beer, K. Harre, T. Pabst, W. Kenn, S.
Neubauer, and D. Hahn
**Analysis of First-Pass and Delayed Contrast-Enhancement Patterns
of Dysfunctional Myocardium on MR Imaging: Use in the Prediction of
Myocardial Viability**
Am. J. Roentgenol., June 1, 2000; 174(6): 1737 - 1740.
[Abstract] [Full Text]

American Journal of Roentgenology   ▶HOME

A. J. Duerinckx
Myocardial Viability Using MR Imaging: Is It Ready for Clinical Use?
Am. J. Roentgenol., June 1, 2000; 174(6): 1741 - 1743.
[Full Text]

Radiology   ▶HOME

H. Arheden, M. Saeed, C. B. Higgins, D.-W. Gao, P. C. Ursell, J. Bremerich,
R. Wyttenbach, M. W. Dae, and M. F. Wendland
**Reperfused Rat Myocardium Subjected to Various Durations of
Ischemia: Estimation of the Distribution Volume of Contrast Material
with Echo-planar MR Imaging**
Radiology, May 1, 2000; 215(2): 520 - 528.
[Abstract] [Full Text]

This Article

▶ **Abstract** FREE
▶ **Alert me when this article is cited**
▶ **Alert me if a correction is posted**
▶ **Citation Map**

Services

▶ **Email this article to a friend**
▶ **Similar articles in this journal**
▶ **Similar articles in PubMed**
▶ **Alert me to new issues of the journal**
▶ **Download to citation manager**
▶ **Request Permissions**

Citing Articles

▶ **Citing Articles via HighWire**
▶ **Citing Articles via Google Scholar**

Google Scholar

▶ **Articles by Lima, J. A. C.**
▶ **Articles by Zerhouni, E. A.**
▶ **Search for Related Content**

PubMed

▶ **PubMed Citation**
▶ **Articles by Lima, J. A. C.**
▶ **Articles by Zerhouni, E. A.**

Circulation Home | Subscriptions | Archives | Feedback | Authors | Help | AHA Journals Home | Search